The Astrophysical Journal, 511:666–670, 1999 February 1

RXTE AND *ASCA* CONSTRAINTS ON NONTHERMAL EMISSION FROM THE A2256 GALAXY CLUSTER

Mark Henriksen
Physics Department, University of North Dakota, Grand Forks, ND 58202-7129; mahenrik@plains.NoDak.edu
Received 1998 July 2; accepted 1998 September 4

ABSTRACT

An 8.3 hr observation of the Abell 2256 galaxy cluster using the *Rossi X-Ray Timing Explorer* proportional counter array produced a high-quality spectrum in the 2–30 keV range. Joint fitting with the 0.7–11 keV spectrum obtained with the *ASCA* gas imaging spectrometer gives an upper limit of $\sim 2.3 \times 10^{-7}$ photons cm^{-2} s^{-1} keV^{-1} for nonthermal emission at 30 keV. This yields a lower limit to the mean magnetic field of 0.36 μG and an upper limit of 1.8×10^{-13} ergs cm^{-3} for the cosmic-ray electron energy density. The resulting lower limit to the central magnetic field is $\sim$1–3 μG. While a magnetic field of $\sim$0.1–0.2 μG can be created by galaxy wakes, a magnetic field of several microgauss is usually associated with a cooling flow or, as in the case of the Coma Cluster, a subcluster merger. However, for A2256 the evidence for a merger is weak and the main cluster shows no evidence of a cooling flow. Thus there is presently no satisfactory hypothesis for the origin of an average cluster magnetic field as high as greater than 0.36 μG in the A2256 cluster.

Subject headings: galaxies: clusters: individual (A2256) — galaxies: magnetic fields — intergalactic medium — X-rays: galaxies

1. INTRODUCTION

The Abell 2256 galaxy cluster ($z = 0.058$), like the Coma Cluster, is one of the most studied galaxy clusters. A2256 and the Coma Cluster share many common properties: they both have similar X-ray luminosities, both have optical and X-ray substructure, and both have a radio halo. As with Coma, it has been over 20 yr since the radio halo of A2256 was discovered (Bridle & Fomalont 1976; Bridle et al. 1979). These authors report that the radio halo has a flux of 0.1 Jy at 610 MHz and extends to a radius of 5′, or 0.52 H_0^{-1} Mpc. The spectrum is a power law given by $S = 6.5 \times 10^{-9} \nu^{-1.8}$ ergs cm^{-2} s^{-1} Hz^{-1}. The spectral index is determined to be between 610 and 1415 MHz. As with Coma, the radio spectrum is attributed to synchrotron emission from a population of relativistic electrons interacting with a diffuse intergalactic magnetic field. Recent studies of the Coma Cluster link the X-ray and radio emission to support the hypothesis that the merger amplifies the magnetic field. However, for A2256 this hypothesis may not work since the evidence for a merger is incomplete; there is evidence of substructure, yet shock heating due to the merger is not as apparent in the temperature map obtained with *ASCA* (Markevitch & Vikhlinin 1997) as it is for Coma.

X-ray emission is also expected from inverse Compton scattering of cosmic microwave photons off of the relativistic electrons that produce the radio halo. So far, attempts to detect nonthermal emission have only produced upper limits for both clusters. Previous searches for nonthermal emission from A2256 have utilized hard X-ray data obtained with HEAO 1 A-4 (Rephaeli, Gruber, & Rothschild 1987). An upper limit to the nonthermal X-ray flux reported from this study is 5×10^{-6} photons cm^{-2} s^{-1} keV^{-1} at 30 keV. The lower limit to the average magnetic field of A2256 is 0.11 μG.

The alternative hypothesis to mergers, that galaxy wakes amplify a seed field, leads to an average field in the range of 0.1–0.2 μG (Goldman & Rephaeli 1991). If this hypothesis is correct, nonthermal emission should be detectable for A2256 with even a slight improvement in sensitivity over the HEAO 1 A-4 X-ray spectrum. In this paper we use the very high signal-to-noise data obtained with the *ASCA* gas imaging spectrometer (GIS) combined with that obtained with the *Rossi X-Ray Timing Explorer* (*RXTE*) proportional counter array (PCA) to place a more sensitive limit on the nonthermal X-ray emission from the A2256 cluster. This new limit provides a more stringent constraint on current hypotheses for its origin. A value of 50 km s^{-1} Mpc^{-1} is used throughout this paper.

2. OBSERVATIONS

The A2256 cluster was observed with *RXTE* on 1997 June 24–26 for 30,000 s. Data obtained with the PCA is analyzed and presented here. The PCA consists of five proportional counter units (PCU), each of which contains three detector layers. The nominal energy band of the PCA is 2–60 keV. After filtering the PCA data, there were $\sim$22,000 s of good data. Filtering involved excluding data when fewer than 5 PCUs were on (this eliminated less than 1000 s), excluding data taken when the pointing was greater than 0°.02 offset from the source, excluding data taken less than 10° elevation from the Earth, and excluding times near passage through the South Atlantic Anomaly that showed large variations in the count rate. The observation was carried out in two observing periods, each resulting in $\sim$11,000 s of filtered data. Modeled spectra include: spectra obtained for the top layer detectors alone for each observation period, both separate and combined, and the top and middle layer detectors. The background was modeled using the latest models available from the *RXTE* guest observer facility. The background estimation is based on three models: VLE (based on the rate of very large event discriminator), activation, and cosmic X-ray background. The VLE background results from interaction of cosmic rays with the spacecraft or detector and unvetoed cosmic-ray tracks. The activation model depends on orbital coordinates and corrects for additional background associated with passes from the South Atlantic Anomaly. The cosmic

X-ray background component is derived from blank sky observations taken in 1997 to give an average high-latitude X-ray background spectrum.

The model background consists of the VLE and activation components (in which sky background is included from blank sky observations). In the third layer, the 30–60 keV range, little source emission should be present. Indeed, the count rate in the 2–30 keV range between the first and second layer drops by a factor of ~ 15, and the ~ 7 keV thermal continuum, which characterizes the A2256 X-ray spectrum, contributes little emission above 30 keV. The model background is fitted to the 30–60 keV spectrum while normalizing the activation component separately to minimize χ^2.

The 2–30 keV part of the spectrum used in the model fitting utilizes the background derived by this procedure. The best constraint on the nonthermal flux was obtained by fitting data obtained in the top and second layers in the first 11 ks observing period. The background-subtracted count rates for the data analyzed are 28.43 ± 0.23 counts s^{-1} in the top layer of the PCA, 1.91 ± 0.07 counts s^{-1} in the second layer, and 1.16 ± 0.05 counts s^{-1} in the third layer.

The spectral response of the PCA depends on the overall gain setting, which PCUs are analyzed since they have different gains, and the detector layer. Separate response matrices were created for each detector layer of each PCU used. The matrices were binned to the 129 channel, standard two configuration in which the data were analyzed. There is a feature in the response from the detector due to the Xenon ledge at 4.78 keV, which produces an absorption feature in the spectrum. Ignoring channels 10–11 in the PCA greatly reduces the residuals in this part of the spectrum; this is done in all of the model fitting that involves the PCA.

The *ASCA* GIS spectrum consists of 34,726 s of good data with a count rate of 1.57 ± 0.007 counts s^{-1}. Preparation of the GIS spectrum and related calibration issues are discussed in detail in Henriksen (1998).

3. ANALYSIS AND RESULTS

The models fit to the data consist of one or two Raymond & Smith (1977, hereafter RS) thermal components with and without a power-law component. For the thermal components, all of the data groups share the following free parameters: column density, temperature, and abundance. The normalization(s) for the PCA data sets are tied while the GIS has its own normalization(s). The power-law component has a free normalization and the spectral index is fixed at the photon index measured from the radio, 2.8, which is also the spectral index of the inverse Compton component. Both the GIS and the PCA field of view contain the region of the radio halo so that their power-law normalizations are tied. Thus for the joint data fits there are six free parameters for the single RS component plus a power law, and eight free parameters for the model consisting of two RS components and a power law. The 90% range on fit parameters are given in Tables 1 and 2 for each data set alone and the joint fit. When addition of a power law improves χ^2, the fit is also shown without the power law to make the significance of the additional component apparent.

The addition of a second temperature component is significant with the PCA data alone, as well as in the joint fit with the GIS data. This is not a surprising feature of the

TABLE 1

RESULTS OF SINGLE AND JOINT FITS

Model	Data Set	n_H ($\times 10^{22}$ cm^{-2})	kT (keV)	Abundance	NT Normalization[a]	χ^2/dof
1 RS	GIS	0.028–0.061	6.78–7.44	0.16–0.24	<0.0045	633.0/604
1 RS	PCA	0.042[b]	6.63–6.81	0.15–0.18	...	172.6/114
1 RS + POW	PCA	0.042[b]	7.10–7.43	0.23–0.27	0.0091–0.015	127.6/113
1 RS	Joint	0.042–0.066	6.66–6.84	0.16–0.18	...	815.8/720
1 RS + POW	Joint	0.091–0.18	6.79–7.08	0.18–0.22	0.0019–0.0087	806.7/719
2 RS	PCA	0.042[b]	6.97–7.59	0.18–0.24	<0.0082	122.5/113
			0.71–1.71			
2 RS	Joint	0.029–0.11	6.99–7.38	0.19–0.23	<0.0032	756.0/717
			0.75–1.46			

[a] Nonthermal upper limit in photons cm^{-2} s^{-1} keV^{-1} at 1 keV.
[b] n_H is fixed at the Galactic value, 0.042.

TABLE 2

RESULTS OF JOINT FITS

		NORMALIZATION		FLUX	
MODEL	DATA SET	High T	Low T	High T[a]	Low T[a]
1 RS	GIS	0.087–0.089	...	7.81	...
	PCA	0.071–0.073	...	6.36	...
1 RS + POW	GIS	0.078–0.085	...	6.89	...
	PCA	0.063–0.066	...	5.78	...
2 RS	GIS	0.084–0.087	0.00–0.011	7.97	0.00
	PCA	0.063–0.068	0.024–0.077	6.12	0.31

[a] Multiplied by 10^{-11} ergs cm^{-2} s^{-1} keV^{-1} in the 2–10 keV band. Flux is derived from best fitting normalization.

integrated spectrum since a temperature map of the cluster shows multiple components (Markevitch & Vikhlinin 1997; Miyaji et al. 1993). The addition of the second cooler component provides much improvement in the joint fit; $\Delta\chi^2$ decreases by 60 for 3 additional degrees of freedom. The parameters derived from fitting the GIS data and the PCA data separately are in very good agreement, which suggests the data are independently well calibrated. The PCA data alone do not constrain the Galactic column density, so this parameter is tied at the value measured from neutral hydrogen, 4.2×10^{20}.

The PCA data alone are consistent with a detection of nonthermal emission when a power law is added to a single thermal component. However, addition of a second thermal component rather than the power law provides an even better fit to the data. Addition of a power law to the two thermal components then degrades the fit, and the data provide an upper limit on nonthermal emission. The joint fit with the GIS also shows that a second thermal component provides a much better fit than does a power law. The joint fit of two RS models also then gives the best upper limit on nonthermal emission (see Fig. 1). The upper limit on the nonthermal flux obtained from the joint fit, 2.64×10^{-12} ergs cm^{-2} s^{-1} in the 2–10 keV band, is $\sim$24 times better than that obtained by HEAO 1 A-4.

The *RXTE* PCA temperature alone is 6.63–6.81 keV, which is in good agreement with the *ASCA* GIS measurement, 6.78–7.44 keV, and measurements by previous X-ray observations: the *Einstein* MPC (6.7–8.1 keV; David et al. 1993) and *Ginga* (7.32–7.70 keV; Hatsukade 1989). The abundance obtained from *RXTE*, 0.15–0.18, is consistent with *ASCA*, which measured 0.16–0.24. This general agreement with past measurements suggests that the spectral calibration of the PCA is accurate within the energy band used here.

The HEXTE observations were also analyzed. Adding the HEXTE spectrum did not constrain the models beyond that obtained by fitting only the PCA and the GIS.

The best-fit model, which consists of two thermal components, was refit to assess the impact of cosmic X-ray background (CXB) fluctuations in the PCA detector field. The procedure for estimating the positive and negative amplitude flux is given in Valinia et al. (1999). Refitting gives an upper limit on the nonthermal flux of 0.0022 photons cm^{-2} s^{-1} keV^{-1} at 1 keV for the positive fluctuation, and 0.0042 photons cm^{-2} s^{-1} keV^{-1} for the negative fluctuation. The lower limit to the average magnetic field calculated from this nonthermal flux upper limit is 0.33 μG. Refitting with inclusion of the CXB fluctuation has increased the nonthermal upper limit by 30% and decreased in the magnetic field lower limit by 8%. Thus for A2256 the results are only marginally affected by inclusion of the CXB fluctuations.

4. CALCULATION OF $\langle B \rangle$ AND U_r

The average magnetic field, $\langle B \rangle$, is calculated from the radio spectrum and the X-ray flux upper limit using the equations in Henriksen (1998). This procedure combines the expressions for the synchrotron flux and the Compton flux to eliminate the relativistic electron density to obtain

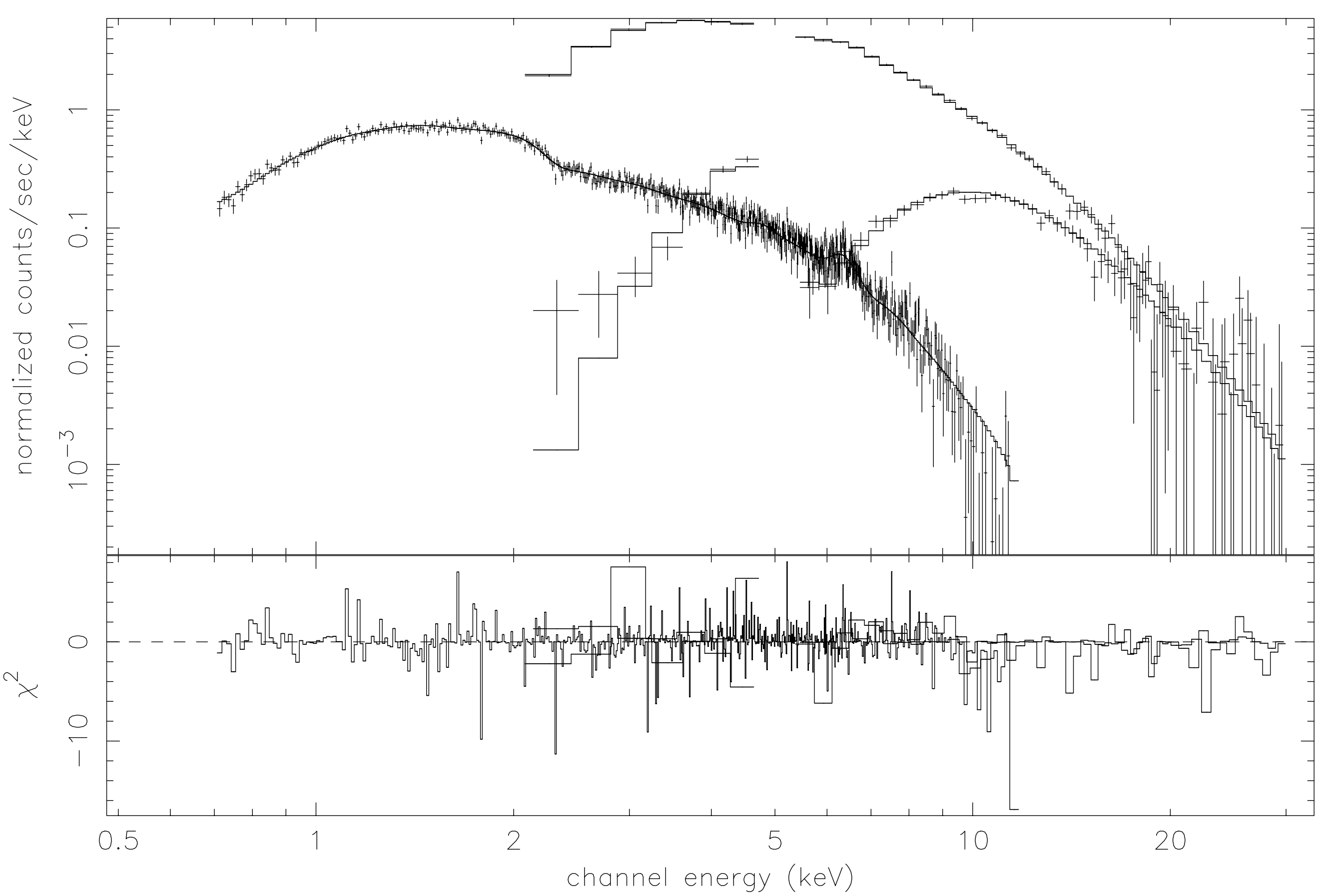

FIG. 1.—Best-fit model for joint fit to *ASCA* GIS and *RXTE* PCA data shown with a power-law component added at the 90% confidence upper limit.

TABLE 3

CALCULATED PARAMETERS

Model	Data Set	NT Flux[a]	$\langle B \rangle$ (μG)	U_r[b]	U_B[c]
1 RS……	GIS	<3.64	>0.30	<2.55	>3.58
	PCA	7.5–12.5	0.20–0.25	5.3–8.6	1.6–2.5
	Joint	1.58–7.09	0.25–0.43	1.1–5.0	2.5–7.4
2 RS……	PCA	<6.80	>0.25	<4.8	>2.5
	Joint	<2.64	>0.36	<1.8	>5.2

[a] Nonthermal flux multiplied by 10^{-12} ergs cm^{-2} s^{-1} in the 2–10 keV band.

[b] Electron energy density multiplied by 10^{-13} ergs cm^{-3}.

[c] Magnetic field energy density multiplied by 10^{-15} ergs cm^{-3}.

an expression that is independent of the size of the emitting region or the distance to the cluster. The derived values of $\langle B \rangle$ are given in Table 3. The highest lower limit is 0.36 μG. An upper limit to the energy density of relativistic electrons is calculated using the equation

$$U_r = C \int (\gamma E) \gamma^{-p} d\gamma \ . \tag{1}$$

In this equation, U_r is the relativistic electron energy density, γ is the Lorentz factor, E is the electron rest energy, and C and p are defined by the relativistic electron density distribution

$$n(\gamma) = C\gamma^{-p} \ . \tag{2}$$

The lower limit on the integral is the minimum γ needed to boost a cosmic microwave background radiation photon to the X-ray regime, 1000. Solving the integral gives

$$U_r = \frac{CE\gamma_{\min}^{2-p}}{p-2} \ . \tag{3}$$

The spectral index of the relativistic electrons (p) is related to the photon index used to model the inverse Compton emission ($\alpha_x = 2.8$) by $p = 2\alpha_x - 1$. The parameter C is calculated by multiplying equation (4) of Henriksen (1998), which is the expression for the inverse Compton energy density in terms of various constants, by the volume containing the relativistic electrons that is taken to be a sphere with radius equal to that of the radio halo. This equation is then divided by $4\pi D^2$, where D is the distance to the cluster to get the inverse Compton flux. The inverse Compton flux, given in Table 3 in the 2–10 keV energy band, is the primary observational constraint in this calculation. The calculated upper limits on U_r are given in Table 3. The magnetic field energy density is calculated for comparison and shown in Table 3. In all cases, the energy density in cosmic rays and the magnetic field are consistent with equipartition.

5. DISCUSSION

A joint fit of the GIS and PCA data in the 0.7–30 keV band shows that the A2256 spectrum is best described by a model consisting of two thermal components. Using a single thermal component leads to a detection of nonthermal emission. However, a second thermal component provides a better description of the data and obviates the need for nonthermal emission. These data place a more stringent upper limit on the flux of nonthermal emission, less than 2.64×10^{-12} ergs cm^{-2} s^{-1} in the 2–10 keV band, or less than 4% of the thermal component. From the upper limit on nonthermal emission, a lower limit to the average magnetic field is calculated to be 0.36 μG. If the field is assumed to be frozen into the intracluster gas, then the central field will be higher. Using the gas density parameters for A2256 (Jones & Forman 1984) and the formulae in Goldshmidt & Rephaeli (1994), a central field of $\gtrsim$1–3 μG is calculated. The range corresponds to using the radio halo or the intracluster medium for the average magnetic field extent. Using these parameters (central gas density equals 2.5×10^{-3} cm^{-3}) and the ambient gas temperature of 7 keV gives a central gas energy density of 3×10^{-11} ergs cm^{-3}. The highest lower limit to the magnetic field energy density at the center, greater than 3.6×10^{-13}, is almost a factor of $\sim$83 lower. The energy density in cosmic-ray electrons, less than 1.8×10^{-13}, is also much lower. This gives an indication of the relative importance of the magnetic field and cosmic-ray electrons on the gas dynamics of the cluster. The cosmic-ray energy is not significant. The magnetic field energy is a lower limit and not constraining. Detection of an average magnetic field that gives a comparable energy density to the gas at the center would require an increase in sensitivity in X-ray flux of $\sim$470.

The hypothesis that galaxy wakes amplify a seed field via the dynamo process leads to an average field of 0.1–0.2 μG (Goldman & Rephaeli 1991). These authors use a lower, more realistic efficiency for the conversion of kinetic energy into magnetic field energy than earlier studies that produced a field of $\sim$2 μG (Ruzmaikin, Sokoloff, & Shukarov 1989). Amplification for seed fields has also been considered by De Young (1992) using time-dependent evolution of magnetohydrodynamic turbulence from galaxy wakes. He found that amplification to a few microgauss with this mechanism is very rare. Magnetic field strengths of a few microgauss have previously been inferred from studies of the excess rotation measure (Kim et al. 1990; Crusius-Watzel et al. 1990; Kim, Kronberg, & Tribble 1991) in galaxy clusters. Although these high magnetic fields challenge the hypothesis of wake amplification, they are more model dependent since they are sensitive to local density inhomogeneities or an asymmetric gas distribution; clusters often have both due to accretion of groups and subcluster mergers. In addition, many other clusters also have cooling flows that can amplify the magnetic field through isotropic compression (Soker & Sarazin 1990; Tribble 1991). The distribution of excess rotation measures for Abell clusters found by Kim et al. (1991) is consistent with amplification by galaxy wakes if $\sim$10% have cooling flows that further amplify the magnetic fields (Carvalho 1994). However, this requires that clusters with the larger magnetic fields greater than 0.1–0.2 μG be those clusters with cooling flows. Based on a deprojection analysis of its X-ray emission, A2256 does not have a cooling flow (Stewart et al. 1984) and does not show the surface brightness central excess, which is typical of clusters with cooling flows (Jones & Forman 1984).

As an alternative, Tribble (1993) has suggested that cluster mergers have amplified the magnetic fields in clusters with radio halos. This hypothesis has received support in subsequent studies of the radio halo in Coma, which suggests that it may be maintained by the recent merger experienced in the cluster center that is apparent in the X-ray (Deiss et al. 1997). Bohringer et al. (1992) find that the available energy specifically from the accretion of groups near the core may be enough to reaccelerate cosmic-ray electrons and amplify the magnetic field to maintain the halo; however, this hypothesis presents a problem in the case of A2256 because the evidence for a merger is controversial. The pattern of heating expected in a merger has been found in several of the clusters (Coma, A754, and A1367). Nonisothermality in the atmosphere of A2256 was reported using *ROSAT* PSPC data (Briel & Henry 1994), Broad Band X-Ray Telescope data (Miyaji et al. 1993), and *ASCA* (Markevitch & Vikhlinin 1997). However, Miyaji et al. (1993) found that the temperature map was consistent with the superposition of two subclusters with different temperatures rather than a merger. Future observation of A2256 by the *Advanced X-Ray Astrophysics Facility* (*AXAF*) will likely provide a more definitive description of the dynamical state of the cluster. Thus a satisfactory hypothesis for the origin of an average magnetic field greater than 0.4 μG in A2256 is not yet apparent.

I thank the National Science Foundation for supporting this research. I also thank the referee for comments on improving this manuscript.

REFERENCES

Bohringer, H., Schwarz, R., Briel, U., Voges, W., Ebeling, H., Hartner, G., & Cruddace, R. 1992, in Clusters and Superclusters of Galaxies, ed. A. Fabian (NATO/ASI), 71
Bridle, A., & Fomalont, E. 1976, A&A, 52, 107
Bridle, A., Fomalont, E., Miley, G., & Valentijn, E. 1979, A&A, 80, 201
Briel, U., & Henry, J. 1994, Nature, 372, 439
Carvalho, J. C. 1994, A&A, 281, 641
Crusius-Watzel, A., Biermann, P., Lerche, I., & Schlickeiser, R. 1990, ApJ, 360, 417
David, L. P., Slyz, A., Jones, C., Forman, W., Vrtilek, S. D., & Arnaud, K. A. 1993, ApJ, 412, 479.
Deiss, B., Reich, W., Lesch, H., & Wielebinski, R. 1997, A&A, 321, 55
De Young, D. 1992, ApJ, 386, 464
Goldman, I., & Rephaeli, Y. 1991, ApJ, 380
Goldshmidt, O., & Rephaeli, Y. 1994, ApJ, 431, 586
Hatsukade, I. 1989, Ph.D. thesis, Osaka Univ.
Henriksen, M. E. 1998, PASJ, 50, 389
Jones, C., & Forman, W. 1984, ApJ, 276, 38
Kim, K.-T., Kronberg, P. P., Dewdney, P. E., & Landecker, T. L. 1990, ApJ, 355, 29
Kim, K.-T., Kronberg, P. P., & Tribble, P. C. 1991, ApJ, 379, 80
Markevitch, M., & Vikhlinin, A. 1997, ApJ, 474, 84
Miyaji, T., et al. 1993, ApJ, 419, 66
Raymond, J., & Smith, B. 1977, ApJS, 35, 419 (RS)
Rephaeli, Y., Gruber, D., & Rothschild, R. 1987, ApJ, 320, 139
Ruzmaikin, A., Sokoloff, D., & Shukarov, A. 1989, MNRAS, 241, 1
Soker, N., & Sarzin, C. 1990, ApJ, 348, 73
Stewart, G., Fabian, A., Jones, C., & Forman, W. 1984, ApJ, 285 1
Tribble, P. 1991, MNRAS, 248, 741
———. 1993, MNRAS, 263, 31
Valinia, A., Henriksen, M., Loewenstein, M., Roettiger, K., Mushotzky, R., & Madejski, G. 1999, ApJ, in press